SAJET

South Asian Journal of Engineering and Technology Vol.2, No.2 (2016) 173–185

ISSN No: 2454-9614

Retinal Disease Diagnosing from Scanning Laser Ophthalmoscope (SLO) Images

Manickam T, Robini P*,Sri Kowsalya M, S.Sugirtha, M.Supriya

Department Of Electronics and Communication Engineering, Nandha college of Engineering, Erode, Tamilnadu, India.

*Corresponding Author: T.Manickam

E-mail:

Received: 10/11/2015, Revised: 11/12/2015 and Accepted: 04/03/2015

Abstract

Early detection and treatment of retinal eye diseases is critical to avoid preventable vision loss. Digital retinal imaging is widely used to identify patients with retinal disease in primary care. With the advent of the latest screening technology, the advantage of using ultra wide field scanning-laser ophthalmoscope (SLO) is its wide field of view of the retina making it a valuable tool in the management of patients with retinal disease. One consequence of the wide field imaging process is that artefacts such as eyelashes, eyelids and dust on optical surfaces are also imaged along with the retinal area.

Reviewed by* **ICETSET'16 *organizing committee*

1. Introduction

To the best of our knowledge, there is no existing work related to automated differentiation between the true retinal area and these artefacts in an SLO image. The purpose of performing this study is to develop a method that can exclude artefacts in SLO images so as to improve automatic detection of retina diseases. In this paper, we propose a novel approach to automatically extract true retinal area from an SLO image based on image processing and machine learning approaches. To reduce the computational complexity of the image processing tasks and to provide a convenient primitive image pattern, we have grouped pixels into regions based on their regional size and compactness, called super pixels. Image based features representing textural and structural information are calculated and are used to classify the super pixels as retinal area and artefacts. The experimental evaluation results have shown good performance with an overall accuracy of 92% on both healthy and diseased retinal scans compared to clinical annotations. The proposed approach enables effective analysis of retinal area and would have applications that include registering multi-view images into a montage and automated

disease diagnosis.

Fig. 1. Example of a fundus image and an SLO image annotated with true retinal area and ONH.

In this study, we have constructed a novel framework for the extraction of retinal area in SLO images. The three main steps for constructing our framework include:

1) Determination of features that can be used to distinguish between the retinal area and the artefacts;
2) Selection of features which are most relevant to the classification;
3) Construction of the classifier which can classify out the retinal area from SLO images.

2.Literature Survey

Our literature survey is initiated with the methods for detection and segmentation of eyelids and eyelashes applied on images of the front of the eye, which contains the pupil, eyelids, and eyelashes. On such an image, the eyelashes are usually in the form of lines or bunch of lines grouped together. Therefore, the first step of detecting them was the application of edge detection techniques such as Sobel, Prewitt, Canny, Hough Transform **[3]**, and Wavelet transform **[4]**. The eyelashes on the iris were then removed by applying nonlinear filtering on the suspected eyelash areas **[5].** Since eyelashes can be in either separable form or in the form of multiple eyelashes grouped together, Gaussian filter and Variance filter were applied in order to distinguish among both forms of eyelashes **[6].** The experiment showed that separable forms of eyelashes were most likely detected by applying Gaussian filter, whereas Variance filters are more preferable for multiple eyelash segmentation **[7].** Initially, the eyelash candidates were localized using active shape modeling, and then, eight-directional filter bank was applied on the possible eyelash candidates. All of these methods have been applied on CASIA database **[10],** which is an online database of Iris images. In an image obtained from SLO, the eyelashes show as either dark or bright region compared to retinal area depending upon how laser beam is focused as it passes the eyelashes. The eyelids show as reflectance region with greater reflectance response compared to retinal area. Therefore, we need to find out features, which can differentiate among true retinal area and the artefacts in SLO retinal scans. After visual observation, the features reflecting the textural and structural difference could have been the suggested choice. These features have been calculated for different regions in fundus images, mostly for quality analysis.

The characterization of retinal images were performed in terms of image features such as intensity, skew

ness, textural analysis, histogram analysis, sharpness, etc., **[1], [11], [12]**. Dias *et al***. [13]** determined four different classifiers using four types of features. They were analyzed for the retinal area including color, focus, contrast, and illumination. The output of these classifiers were concatenated for quality classification. For classification, the classifiers such as partial least square (PLS) **[14]** and support vector machines (svms) **[15]** were used. PLS selects the most relevant features required for classification. Apart from calculating image features for whole image, grid analysis containing small patches of the image has also been proposed for reducing computational complexity **[11].** For determining image quality, the features of region of interest of anatomical structures such as optic nerve head (ONH) and Fovea have also been analyzed **[16].** The features included structural similarity index, area, and visual descriptor etc. Some of the above mentioned techniques suggest the use of grid analysis, which can be an time effective method to generate features of particular region rather than each pixel. But grid analysis might not be an accurate way to represent irregular regions in the image. There-fore, we decided the use of super pixels **[17]–[20],** which group pixels into different regions depending upon their regional size and compactness.

3.Materials And Methodology

3.1Image Acquisition

To evaluate the performance of this method, the digital retinal images were acquired using digital camera known as Ophthalmoscope. This diagram shows the input image. Fundus image is the interior surface of the eye, opposite the lens, and includes the retina, optic disc, macula, blood vessels and fovea. We tested and evaluated our proposed algorithm on several fundus images. The image set contains both normal and abnormal cases.

Input image

3.2Pre-Processing

Pre-processing stage can be regarded as the bedrock of this work. The aim of pre-processing is to attenuate the noise, to improve the contrast and to correct the non-uniform illumination. Pre-processing mainly includes following stages:

3.3Intensity Conversion:

In digital image processing, images are either indexed images or RGB (Red, Green, Blue) images. In the RGB

images the green channel exhibits the best contrast between the vessels and background while the red and blue ones tends to be more noisy. Hence intensity conversion of image is done using green channel, as the retinal blood vessels appears darker in gray image.

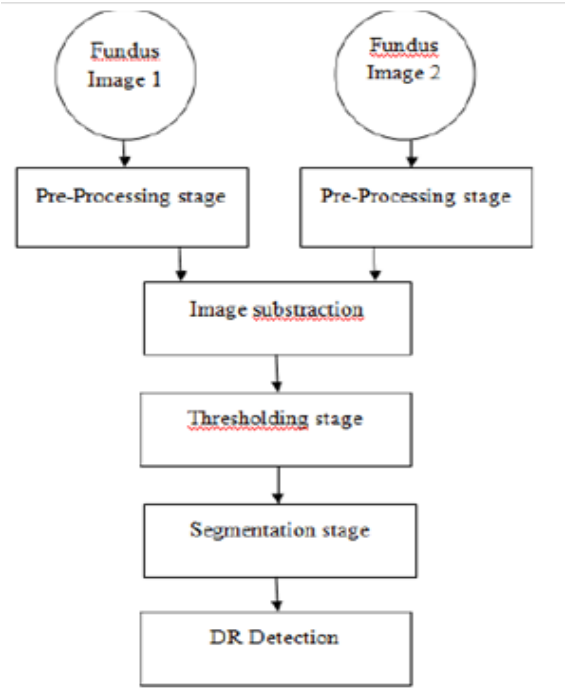

3.3Filtering:

Filtering is used to suppress the unwanted noise which gets added into the fundus image. Here median filtering is used as it is very robust and has the capability to filter any outliers and is an excellent choice for removal of salt and pepper noise.

3.4Adaptive Histogram Equalization

Histogram equalization is performed to improve the image quality. Histogram equalization is nothing but a finding of cumulative distribution function for a given probability density function. After the transformation, the image will have an increased dynamic range, high contrast and probability density function of the output will be uniform. Instead of using normal histogram equalization, adaptive histogram equalization is used as it operates on small regions in the image which are called tiles. Adaptive histogram combines neighbouring tiles using bilinear interpolation to eliminate artificially induced boundaries.

3.5Labeling

Connected components are labelled by scanning an image pixel by pixel in order to identify connected pixel regions. It groups its pixels into components based on pixels connectivity. After group formation each group is

labelled with different color.

3.6*Image Subtraction*

Image subtraction or pixel subtraction is a process were by the digital numeric value of one pixel or whole image is subtracted from another image.

This is primarily done for one of the two reasons leveling uneven section of an image such as half an image having a shadow on it, or detecting changes between two images. This detection of changes can be used to tell if something in the image moved. This is commonly used in field such as astrophotography.

3.7Thresholding:

Thresholding is a method of segmenting image based on the pixel intensity value. Thresholding is used to convert an intensity image to a binary image. Otsu's method is used to automatically perform histogram shape-based image thresholding. Otsu's method chooses the threshold to minimize the interclass variance.

Thresholding is the process of converting a gray scale input image to a bi level image by using an optimal threshold.

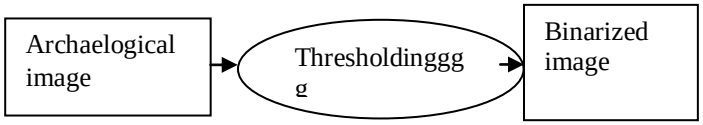

The purpose of thresholding is to extract those pixels from some image which represent an object. Though the information is binary the pixels represent a range of intensities. Thus the objective of binarization is to mark pixel that belong to true foreground regions with different intensities.

3.8Segmentation:

The main objective of segmentation is to group the image into regions with same characteristics. The goal of the segmentation is to simplify and /or change the representation of an image into something that is more meaningful and easier to analyze. Image segmentation is typically used to locate objects and boundaries (lines, curves etc.) in the images. The result of image segmentation is a set of segments that collectively cover the entire image, or a set of contours extracted from the image.

After performing all above operations on the fundus image blobs are detected which is the sign of severe diabetic retinopathy. Also for the mild severity, we used image subtraction algorithm in which earlier and present fundus image is subtracted to detect the new increased blood vessels. Image segmentation is a process of dividing an image into multiple parts. This is typically used to identify objects or other relevant information in digital images. Here K-means algorithm is used.

3.9K-Means Algorithm:

K-means is one of the simplest, unsupervised learning algorithms that solve the well known clustering

problem. The procedure follows a simple and easier way to classify a given data set through a number of clusters. The main idea is to define k centers, one for each cluster. These centers should be placed in a cunning way because of different location causes different results so the better choice is to place them as much as possible far away from each other.

Segmentation Using K-Means Algorithm

1. K-Means is a least-squares partitioning method that divide a collection of objects into K groups. The algorithm iterates over two steps: Compute the mean of each cluster.
2. Compute the distance of each point from each cluster by computing its distance from the corresponding cluster mean. Assign each point to the cluster it is nearest to.
3. Iterate over the above two steps till the sum of squared within group errors cannot be lowered any more.

The initial assignment of points to clusters can be done randomly. In the course of the iterations, the algorithm tries to minimize the sum, over all groups, of the squared within group errors, which are the distances of the points to the respective group means. Convergence is reached when the objective function (i.e., the residual sum-of-squares) cannot be lowered any more. The groups obtained are such that they are geometrically as compact as possible around their respective means. Using the set of feature images, a feature vector is constructed corresponding to each pixel ($\underline{\lfloor e_1(a,b) \rfloor}$, $\underline{\lfloor e_2(a,b) \rfloor}$, ... , $\underline{\lfloor e_d(a,b) \rfloor}$), where d is the number of feature images used for the segmentation process. The K-Means can then be used to segment the image into three clusters - corresponding to two scripts and background respectively. For each additional script, one more cluster is added. Once the image has been segmented using the K-Means algorithm, the clustering can be improved by assuming that neighboring pixels have a high probability of falling into the same cluster. Thus, even if a pixel has been wrongly clustered, it can be corrected by looking at the neighboring pixels.

3.10Description

Given a set of observations ($\mathbf{x}_1$, $\mathbf{x}_2$, …, $\mathbf{x}_n$), where each observation is a *d*-dimensional real vector, *k*-means clustering aims to partition the *n* observations into *k* (≤ *n*) sets $\mathbf{S} = \{S_1, S_2, \ldots, S_k\}$ so as to minimize the within-cluster sum of squares (WCSS) (sum of distance functions of each point in the cluster to the K center). In other words, its objective is to find:

$$\arg\min_{\mathbf{S}} \sum_{i=1}^{k} \sum_{\mathbf{x} \in S_i} \|\mathbf{x} - \boldsymbol{\mu}_i\|^2$$

where $\boldsymbol{\mu}_i$ is the mean of points in S_i.

3.11Color-Based Segmentation Using K-Means Clustering:

Steps involved in segmentation process:

- Step 1: Read Image
- Step 2: Convert Image from RGB Color Space to Gray scale

- Step 3: Classify the Colors Using K-Means Clustering
- Step 4: Label Every Pixel in the Image Using the Results from KMEANS
- Step 5: Segment the Nuclei into a Separate Image

4.Feature Generation

After the generation of super pixels, the next step is to determine their features. We intend to differentiate between the retinal area and artefacts using textural, grayscale gradient, and regional based features. Textural and gradient based features are calculated from red and green channels on different Gaussian blurring scales, also known as smoothing scales [23]. In SLO images, the blue channel is set to zero; therefore, no feature was calculated for the blue channel. The regional features are determined for the image irrespective of the color channel. The details of these features are described as follows

1) Textural Features: Texture can be analyzed using Haralick features [24] by gray level co-occurrence matrix (GLCM) analysis. GLCM determines how often a pixel of a gray scale value *i* occurs adjacent to a pixel of the value *j*. Four angles for observing the pixel adjacency, i.e., $\theta = 0^{\circ}, 45^{\circ}, 90^{\circ}, 135^{\circ}$ are used. These directions are shown in Fig. 3(a). GLCM also needs an offset value **D**, which defines pixel adjacency by certain distance. In our case, offset value is set to 1. Fig. 3(b) illustrates the process of creating GLCM using the image **I**. The features, which are calculated using GLCM matrix are summarized in Table I. The mean value in each direction was taken for each Haralick feature and they were calculated from both red and green channels.

2) Gradient Features: The reason for including gradient features was illumination non uniformity of the artefacts. In order to calculate these features, the response from Gaussian filter bank [23] is calculated. The Gaussian filter bank includes Gaussian $N(\sigma)$, its two first-order derivatives $N_x(\sigma)$ and $N_y(\sigma)$ and three second-order derivatives $N_{xx}(\sigma)$, $N_{xy}(\sigma)$, and $N_{yy}(\sigma)$ in horizontal (x) and vertical (y) directions. After convolving the image with the filter bank at a particular channel, the mean value is taken over of each filter response over all pixels of each super pixel.

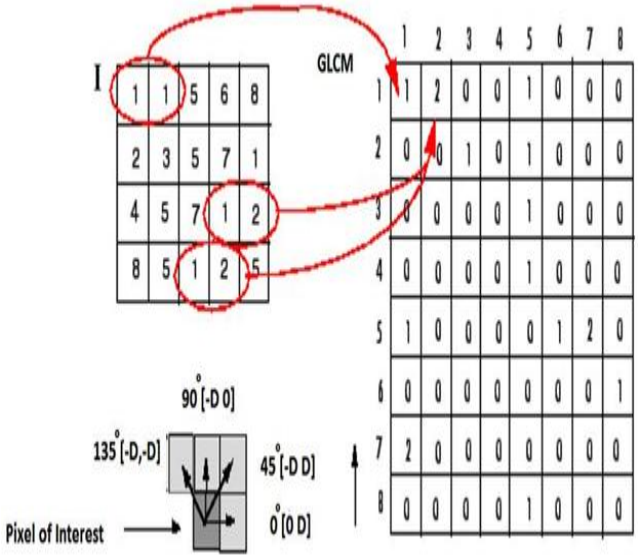

(a) (b)

Fig. 3. (a) GLCM directions and offset. (b) GLCM process using image **I** [25].

3) Regional features: the features used to define regional attributes were included because super pixels belonging artifacts have irregular shape compared to the those belonging the retinal area in an SLO image.

4.*1Feature Selection*

The main purposes for feature selection are reducing execution time, determination of features most relevant to the classification and dimensionality reduction. For feature selection, we have selected sequential forward selection approach. SFS is computationally intensive as it required 5 min/feature on filtered feature set and 30 min/feature on complete feature set. But the results show that the SFS approach performed better compared to other two approaches despite of the fact that the feature set also consists of those features which ranked low in independent evaluation criterion. The Table IV represents the percentage of different types of features selected in each feature set. The table shows clear dominance of textural features compared to gradient features and regional features.

4.2Classsifier Construction:

The classifier is constructed in order to determine the different classes in a test image.in our case, it is a two class problem: true retinal area and artefacts. We have applied Artificial Neural Networks (ANNs). The ANN is the classification algorithm that is inspired by human and animal brain. It is composed of many interconnected units called artificial neurons. ANN takes training samples as input and determines the model that best fits to the training samples using nonlinear regression. Consider the Fig. 6 which shows three basic blocks of ANN, i.e., input, hidden layer (used for recoding or providing representation for input), and output layer. More than one hidden layer can be used but in our case, there is only one hidden layer with ten neurons.

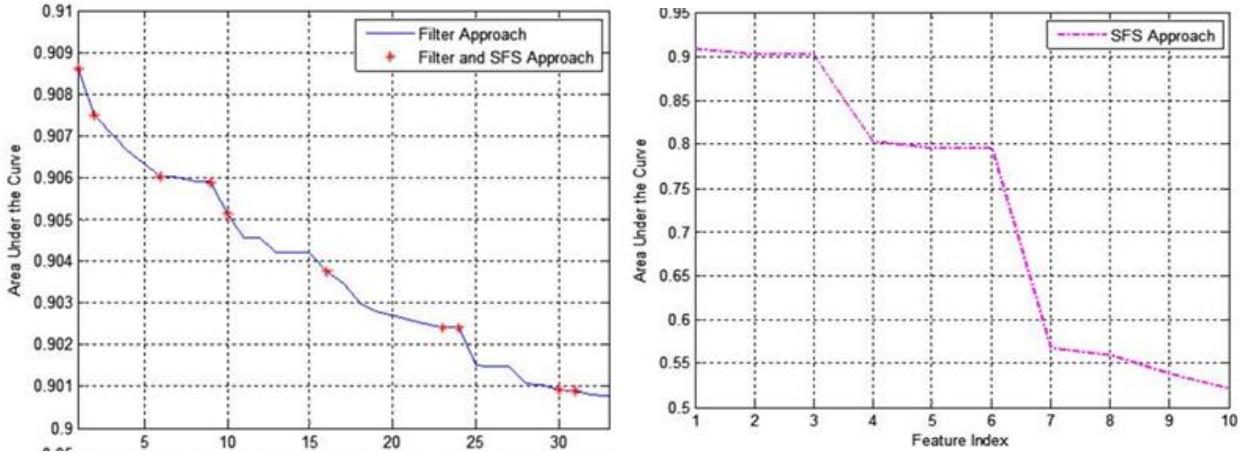

Fig 4.plot of independent evaluation criterion.

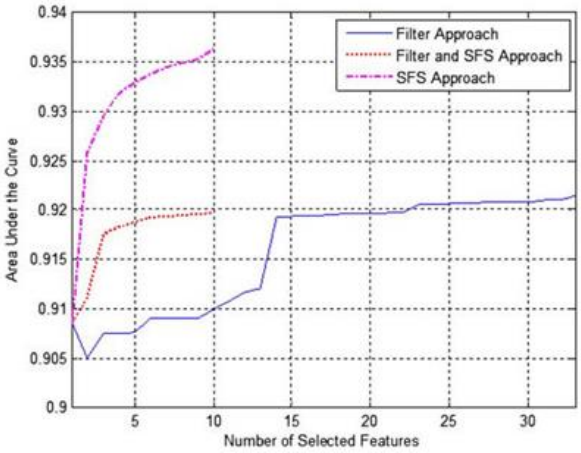

Fig. 5. Plot of AUC by selecting one by one in different feature set.the features

Table I
Percentage Of Different Types Of Features Across Different Feature Set

Feature set	Textural Features	Gradient Features	Regional Features
SFS approach	90 %	10 %	0 %
Filter approach	72.73 %	24.24 %	3.03 %
Filter and SFS Approach	100 %	0 %	0 %

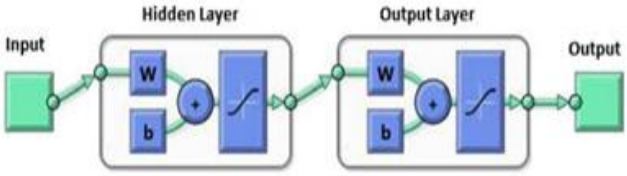

AANs diagram

4.3Experimental Evaluation

Each image has a FOV of up to 200˚ of the retina in a resolution of 14 μm. The device captures the retinal image with-out dilation, through a small pupil of 2 mm. The image has two channels: red and green. The green channel (wavelength: 532 nm) provides information about the sensory retina to retinal pigment epithelium, whereas the red channel (wavelength : 633 nm) shows deeper structures of the retina toward the choroid. Each image has a dimension of 3900 × 3072 and each pixel is represented by 8-bit on both red and green channels. The dataset is composed of healthy and diseased retinal images; most of the diseased retinal images are from Diabetic Retinopathy patients. The system has been trained with 28 images and tested against 76 images.

Fig. 7 compares the classification power of different feature sets with the help of receiver operating characteristics (ROC). One of those feature sets include all features calculated. The rest of other feature sets include features selected by the approaches discussed in Section III-D. By using SFS approach, ten features out of 295 features have been selected and their calculation time is 25 s per image, whereas calculating the complete feature set can take around 10 min per image. The ROC curves and AUC values reveal that if the features are selected using the SFS approach, they can have a classification power almost similar to the complete feature set while reducing the computational time.

The visual results and the accuracies of different classifiers among different feature sets has been presented using Dice Coefficient as evaluation metric. The Dice Coefficient is the degree of overlap between the framework output and the benchmark obtained from the clinician. The Dice Coefficient is defined as

$$D(A, B) = \frac{2|A \cap B|}{|A| + |B|} \quad (1)$$

where A and B are the segmented images obtained from the framework and the benchmark. Let RA_1 and AR_1 represent samples from the retinal area and the artefact area obtained from the framework, respectively, and RA_2 and AR_2 be these samples from the benchmark. The class of super pixels in the benchmark was decided based on majority of pixels in the super pixel belonging to particular class. If we calculate Dice Coefficient for the image, (8) can be deduced as

$$D_I = \frac{(|RA_1 \cap RA_2| + |AR_1 \cap AR_2|)}{N_{\text{sample}}}. \quad (2)$$

The Dice Coefficient for the retinal area D_R and artefacts D_A will be given as

$$D_R = 2|RA_1 \cap RA_2|, \; D_A = 2|AR_1 \cap AR_2|. \quad (3)$$

$\overline{|RA_1| + |RA_2|}$ $\overline{|AR_1| + |AR_2|}$

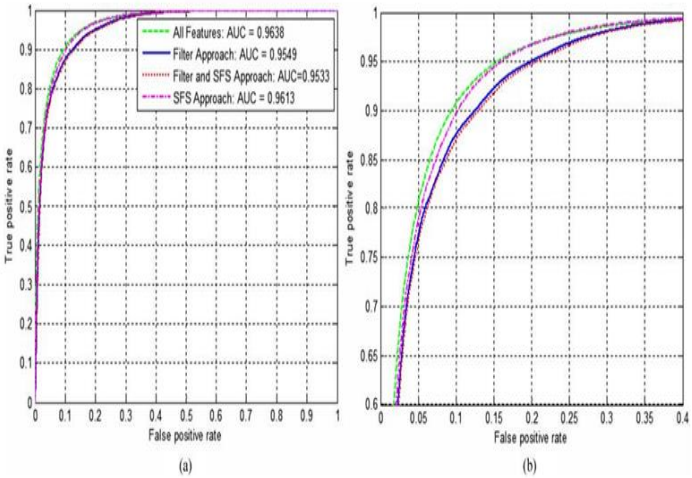

Fig. 7. (a) ROC on the test sets. (b) Magnified version of (a).

5. Discussion And Conclusion

Distinguishing true retinal area from artefacts in SLO images is a challenging task, which is also the first important step to-ward computer-aided disease diagnosis. In this study, we have proposed a novel framework for automatic detection of true retinal area in SLO images. We have used super pixels to represent different irregular regions in a compact way and reduce the computing cost. Feature selection enable the most significant features to be selected and, thus, reduces computing cost too. A classifier has been built based on selected features to extract out the retina area. It has been compared to other two classifiers and was compatible while saving the computational time. The experimental evaluation result shows that our proposed framework can achieve an accuracy of 92% in segmentation of the true retinal area from an SLO image. Feature selection is necessary so as to reduce computational time during training and classification. Among different approaches used for feature selection, the performance of our feature selection approach surpassed the filter approach and "Filter and SFS" approaches in terms of classification po

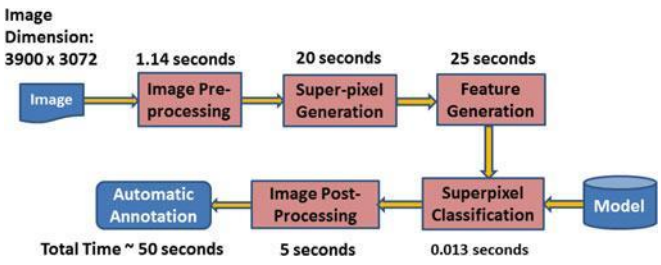

The comparison of different feature selection approaches shows that selection of features based on their mutual interaction can provide the classification power close to that of feature set with all features. Feature selection is once in a life-time process and we can compromise on computational time for feature selection on account of accuracy. As far as the classifier is concerned, the testing time of ANN was the lowest compared to other two classifiers. Although the overall accuracy of SVM was the highest compared to other two classifiers, the training and testing time is quite long. Although *k*NN has the shortest training time, the testing time can be quite high compared to ANN while processing millions of images. Compared to SVM, we can tradeoff the overall accuracy of 0.1% on average while saving the testing time of 8 s per image.

Our retina detection framework serves as the first step toward the processing of ultra wide field SLO images. A complete retinal scan is possible if the retina is imaged from different eye-steered angles using an ultrawidefield SLO and, then, montaging the resulting image. Montaging is possible only if the artefacts are removed before.

6. Acknowledgement

The authors would also like to thank the anonymous reviewers, who provided detailed and constructive comments on an earlier version of this paper.

References

[1] M. S. Haleem, L. Han, J. van Hemert, and B. Li, "Automatic extraction of retinal features from color retinal images for glaucoma diagnosis: A review," *Comput. Med. Imag. Graph.*, vol. 37, pp. 581–596, 2013.
[2] Optos. (2014). [Online]. Available: www.optos.com
[3] R. C. Gonzalez and R. E. Woods, Eds., *Digital Image Processing*, 3rd ed. Englewood Cliffs, NJ, USA: Prentice-Hall, 2006.
[4] M. J. Aligholizadeh, S. Javadi, R. S. Nadooshan, and K. Kangarloo, "Eye-lid and eyelash segmentation based on wavelet transform for iris recogni-tion," in *Proc. 4th Int. Congr. Image Signal Process.*, 2011, pp. 1231–1235.
[5] D. Zhang, D. Monro, and S. Rakshit, "Eyelash removal method for hu-man iris recognition," in *Proc. IEEE Int. Conf. Image Process.*, 2006, pp. 285–288.
[6] A. V. Mire and B. L. Dhote, "Iris recognition system with accurate eyelash segmentation and improved FAR, FRR using textural and topological features," *Int. J. Comput. Appl.*, vol. 7, pp. 0975–8887, 2010.
[7] Y.-H. Li, M. Savvides, and T. Chen, "Investigating useful and distinguish-ing features around the eyelash region," in *Proc. 37th IEEE Workshop Appl. Imag. Pattern Recog.*, 2008, pp. 1–6.
[8] B. J. Kang and K. R. Park, "A robust eyelash detection based on iris focus assessment," *Pattern Recog. Lett.*, vol. 28, pp. 1630–1639, 2007.
[9] T. H. Min and R. H. Park, "Eyelid and eyelash detection method in the normalized iris image using the parabolic Hough model and Otsus thresholding method," *Pattern Recog. Lett.*, vol. 30, pp. 1138–1143, 2009.
[10] Iris database. (2005). [Online]. Available: http://www.cbsr.ia.ac.cn/ IrisDatabase.htm
[11] H. Davis, S. Russell, E. Barriga, M. Abramoff, and P. Soliz, "Vision-based, real-time retinal image quality assessment," in *Proc. 22nd IEEE Int. Symp. Comput.-Based Med. Syst.*, 2009, pp. 1–6.
[12] H. Yu, C. Agurto, S. Barriga, S. C. Nemeth, P. Soliz, and G. Zamora, "Automated image quality evaluation of retinal fundus photographs in diabetic retinopathy screening," in *Proc. IEEE Southwest Symp. Image Anal. Interpretation*, 2012, pp. 125–128.
[13] J. A. M. P. Dias, C. M. Oliveira, and L. A. d. S. Cruz, "Retinal image quality assessment using generic image quality indicators," *Inf. Fusion*, vol. 13, pp. 1–18, 2012.
[14] M. Barker and W. Rayens, "Partial least squares for discrimination," *J. Chemom.*, vol. 17, pp. 166–173, 2003.
[15] J. Paulus, J. Meier, R. Bock, J. Hornegger, and G. Michelson, "Automated quality assessment of retinal fundus photos," *Int. J. Comput. Assisted Radiol. Surg.*, vol. 5, pp. 557–564, 2010.
[16] R. Pires, H. Jelinek, J. Wainer, and A. Rocha, "Retinal image quality analy-sis for automatic diabetic retinopathy detection," in *Proc. 25th SIBGRAPI Conf. Graph., Patterns Images*, 2012, pp. 229–236.
[17] R. Achanta, A. Shaji, K. Smith, A. Lucchi, P. Fua, and S. Susstrunk," "Slic super pixels compared to state-of-the-art superpixel methods," *IEEE Trans. Pattern Anal. Mach. Intell.*, vol. 34, no. 11, pp. 2274–2282, Nov. 2012.

[18] A. Moore, S. Prince, J. Warrell, U. Mohammed, and G. Jones, "Superpixel lattices," in *Proc. IEEE Conf. Comput. Vis. Pattern Recog.*, 2008, pp. 1–8.
[19] O. Veksler, Y. Boykov, and P. Mehrani, "Superpixels and supervoxels in an energy optimization framework," in *Proc. 11th Eur. Conf. Comput. Vis.*, 2010, pp. 211–224.
[20] L. Vincent and P. Soille, "Watersheds in digital spaces: An efficient algorithm based on immersion simulations," *IEEE Trans. Pattern Anal. Mach. Learning*, vol. 13, no. 6, pp. 583–598, Jun. 1991.
T. J. Cheng, J. Liu, Y. Xu, F. Yin, D. Wong, N.-M. Tan, D. Tao, C.-Y. Cheng, T.Aung, and T. Y. Wong, "Super pixel classification based optic disc and optic cup segmentation for glaucoma screening," *IEEE Trans. Med. Imag.*, vol. 32, no. 6, pp. 1019–1032, Jun. 2013.
[22] L. Tang, M. Niemeijer, J. Reinhardt, and M. Garvin, "Splat feature classification with application to retinal hemorrhage detection in fundus images," *IEEE Trans. Med. Imag.*, vol. 32, no. 2, pp. 364–375, Feb. 2013.
Y. M. Abramoff,` W. Alward, E. Greenlee, L. Shuba, C. Kim, J. Fingert, and Y.Kwon, "Automated segmentation of the optic disc from stereo color photographs using physiologically plausible features," *Invest. Ophthalmol. Vis. Sci.*, vol. 48, pp. 1665–1673, 2007.
[23] R. M. Haralick, K. Shanmugam, and I. Dinstein, "Textural features for image classification," *IEEE Trans. Syst., Man, Cybern.*, vol. SMC-3, no. 6, pp. 610–621, Nov. 1973.
[24] R. Haralick and L. Shapiro, Eds., *Computer and Robot Vision*. Reading, MA, USA: Addison-Wesley, 1991.
[25] R. O. Duda, P. E. Hart, and D. G. Stork, Eds., *Pattern Classification*. New York, NY, USA: Wiley-Interscience, 2000.
[26] A. J. Serrano, E. Soria, J. D. Martin, R. Magdalena, and J. Gomez, "Feature selection using ROC curves on classification problems," in *Proc. Int. Joint Conf. Neural Netw.*, 2010, pp. 1–6.
[27] H. Liu and H. Motoda, Eds., *Feature Selection for Knowledge Discovery and Data Mining*. Norwell, MA, USA: Kluwer, 1998.
[28] C.-W. Hsu, C.-C. Chang, and C.-J. Lin, "A practical guide to support vector classification," Dept. Comput. Sci., National Taiwan Univ., Taipei, Taiwan, 2010.